A Molecular Orbital Study of Tambjamine E and Analogues

William J. Skawinski,[†] Thomas J. Venanzi,[‡] and Carol A. Venanzi*[,†]

Department of Chemistry and Environmental Science, New Jersey Institute of Technology, 323 King Blvd., Newark, New Jersey 07102, and Department of Chemistry, College of New Rochelle, New Rochelle, New York 10805

Received: January 16, 2004

Hartree−Fock (HF/6-31G*), electron correlation (MP2/6-31G*, B3LYP/6-31G*, B3LYP/6-31G*(d,p)), and semiempirical (AM1, AM1/SM5.4) calculations were carried out on the DNA AT-specific intercalator tambjamine E in order to investigate the effect of protonation, side chains, electron correlation, and solvent on the inter-ring NCCN rotational barrier and relative planarity of the A and B rings. These properties relate to the flexibility of tambjamine and the ease by which it could adjust its inter-ring twist angle to adopt the propeller twist of DNA in order to form a nonclassical intercalation complex. The E configuration of protonated tambjamine was found to be more stable than the Z due to solvent stabilization and intramolecular hydrogen bonding. Inclusion of electron correlation increased the NCCN rotational barrier by about 2 kcal/mol. Solvent and the presence of the enamine side chain were shown to have a significant effect in lowering the NCCN rotational barrier. For the E configuration of protonated tambjamine, both the Hartree−Fock (HF) and density functional theory (DFT) methods predicted nonplanar minima around 20°, whereas DFT calculated the global energy minimum (GEM) to be planar (180°) in contrast to the HF nonplanar GEM (166°). However, both the HF and DFT results showed that there are broad regions ($\angle$NCCN = 0−30° and 150−180°) in which there is a minimal energetic cost for the E configuration of protonated tambjamine to adopt a nonplanar conformation. Such flexibility of tambjamine around the inter-ring bond could allow the molecule to adjust its NCCN angle to fit the propeller twist of the DNA base pair in order to form a nonclassical intercalation complex.

1. Introduction

DNA sequence selectivity is a basic problem in molecular recognition. Characterization of the molecular structure and properties of the ligand and DNA that determine AT- versus GC-specificity could lead to valuable information on host−guest molecular recognition. Understanding of the interplay of molecular interactions such as stacking, hydrogen bonding, and electrostatic and steric complementarity is relevant not only to the design of novel therapeutic drugs based on AT-specific intercalation, but also to the design of preorganized receptors and other synthetic hosts.[1] Much experimental and theoretical work has been carried out on DNA intercalators with the goal of designing effective anticancer agents[2−7] but most intercalators show GC-sequence specificity and many show no sequence specificity at all. The few monointercalators that exhibit AT sequence specificity are amiloride (Figure 1, top),[8,9] the thiaxanthenones lucanthone,[8,10] hycanthone,[8] and 6-chlorolucanthone,[8,11] several benzothiopyranoindazoles,[11] some naphthothiophene, phenanthrene, and anthracene derivatives,[12] some unfused aromatic cations,[13−20] tambjamine E (referred to subsequently as tambjamine; Figure 1, bottom) and prodigiosen,[21] and piperazinylcarbonyloxyethyl derivatives of anthracene and pyrene.[22] DNA footprinting studies of some of these molecules[11] showed that their preferred DNA binding sequences predominantly consist of alternating A and T residues and that they bind neither to homooligomeric runs of As and Ts nor to regions rich in GC base pairs.

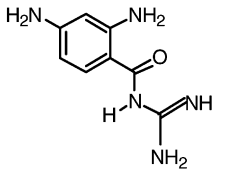

Amiloride

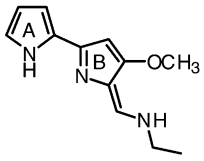

Tambjamine E

Figure 1. Amiloride (top). Tambjamine E (bottom).

Wilson and co-workers found that many unfused polyaromatic cations form a nonclassical intercalation complex which preserves the inter-ring twist angle of the molecule as well as the propeller twist of DNA.[16] In contrast, in a classical intercalation complex between DNA and a planar fused-ring ligand, the DNA propeller twist is severely reduced.[18] Wilson et al.[13,15] designed a series of tricyclic unfused aromatic cations to probe the effect of ligand nonplanarity on DNA binding mode (intercalation versus minor groove binding). They found that molecules with a twist angle less than 20° formed strong intercalation complexes with DNA, even though their structures were more typical of groove binders. Molecules with twist angle greater than 20° did not intercalate.

Amiloride is a sodium channel blocker.[23−26] In previous work from this laboratory, Venanzi and co-workers have been able

* Corresponding author. E-mail: venanzi@adm.njit.edu; Phone: (973) 596-3596; Fax: (973) 596-3596.
[†] New Jersey Institute of Technology.
[‡] College of New Rochelle.

10.1021/jp049758l CCC: $27.50
Published on Web 04/27/2004

to correlate the changes in the molecular structure and molecular electrostatic potential of several amiloride analogues[27−32] to differences in their biological activity as sodium channel blockers.[33,34] Amiloride has also been shown to intercalate into DNA[35] so as to inhibit DNA topoisomerase II. Ab initio calculations[29,28] and NMR studies[36] of the conformational potential energy surface of amiloride by Venanzi and co-workers found amiloride to be a planar molecule with a high barrier for rotation around the C (pyrazine ring) − C (carbonyl group) bond. However, for values of this torsional angle up to approximately 20° out of plane, the conformational energy rises very gradually to about 4 kcal/mol, suggesting that amiloride may have the ability to adjust its C (pyrazine ring) − C (carbonyl group) torsional angle to match the DNA propeller twist.

Electric linear dichroism measurements[8] of amiloride with poly(dA)·poly(dT) and poly(dA-dT)·poly(dA-dT) showed more marked AT selectivity of amiloride for the copolymer. This is in agreement with the DNA footprinting studies[9] that indicate that amiloride prefers to bind to alternating AT sites and that runs of As and Ts are not preferred binding sites. Modeling studies by the Venanzi group have investigated the stacking interaction of amiloride with AT and CG base pairs.[37] Few other calculations have been carried out on complexes of DNA with AT-specific intercalators.[38−40]

Like amiloride, tambjamine is an unfused aromatic bicyclic system, which in its protonated form intercalates into DNA with a preference for AT sites.[21] Unlike amiloride, tambjamine has two small flexible side chains. The present quantum mechanical study was undertaken in order to investigate the effect of the side chains and of solvent on the NCCN rotational barrier, as well as to determine the degree of relative planarity of the A and B rings in the low energy conformers of tambjamine. These properties relate to the flexibility of tambjamine and give an indication of the energetic cost involved in adjusting its inter-ring twist angle to adopt the propeller twist of DNA in order to form a nonclassical intercalation complex. The present work is part of a concerted effort to understand the intermolecular interactions involved in the binding of AT-specific intercalators. Future work will involve modeling the stacking interaction of tambjamine with AT and CG base pairs and NMR and molecular dynamics studies of tambjamine/DNA complexes.

2. Methods

Hartree−Fock and density functional calculations were carried out on tambjamine in vacuo using the Gaussian 98 program[41] on an SGI Origin 2000 at New Jersey Institute of Technology. Both the E (B ring and side chain nitrogens anti to each other, as shown in Figure 1) and Z configurations (B ring and side chain nitrogens syn) were investigated. Hartree−Fock (HF) calculations were carried out using the HF/6-31G* basis set.[42] The A and B rings were individually made planar by holding constant all torsional angles defining ring planarity. All other parameters were allowed to optimize unless otherwise stated. The site of protonation was determined by adding a proton separately to either the side-chain nitrogen or the B-ring nitrogen of the E configuration, and comparing their energies at various values of the NCCN dihedral angle. The structure protonated on the side chain nitrogen was consistently higher in energy (26−38 kcal/mol over the NCCN range) than the B-ring protonated structure. The latter was used for all the HF, DFT, and semiempirical calculations described below.

The NCCN torsional angle between the two rings (∠NCCN) was allowed to vary between 0° and 180° in increments of 30°. Melvin et al.[21] measured the pK_a of the B-ring nitrogen as 10.06, indicating that tambjamine is protonated at physiological pH. To assess the effect of the protonation state on the NCCN rotational barrier, the calculations were carried out on both neutral and protonated tambjamine. However, only for the biologically active protonated form were smaller torsional angle increments and full optimization (variation of the NCCN angle) used to exactly locate the GEM and other nonplanar local minima.

The effect of electron correlation on the rotational barrier and on intramolecular hydrogen bonding was investigated by the use of density functional theory. The NCCN rotational barrier for both neutral and protonated tambjamine in the E configuration was calculated at the B3LYP/6-31G* and B3LYP/6-31G*(d,p) levels.[43] Global and local minima for the protonated species were identified by using the HF/6-31G* minima as starting structures and carrying out full geometry optimization. For comparison purposes, the MP2/6-31G* method was also used to identify minima for this molecule. As in the DFT calculations, the HF/6-31G* minima were used as starting structures for full geometry optimization at the MP2/6-31G* level.

In addition, calculations at the HF/6-31G* level were carried out on "fragment" molecules derived from tambjamine in order to determine the effect of B-ring substitution on the NCCN rotational barrier. No attempt was made to locate nonplanar minima for the fragment molecules (or for neutral tambjamine) by full optimization of the NCCN angle. The following fragment molecules were studied, protonated on the B-ring nitrogen: "proto"-tambjamine (consisting of the A and B rings only with the methoxy and enamine side chains replaced by hydrogens on the B ring), the methoxy analogue (proto-tambjamine with only the methoxy side chain), and the enamine analogue (proto-tambjamine with only the enamine side chain). To form the proto-tambjamine and methoxy analogues, the enamine side chain of tambjamine was removed and two hydrogens were added to the carbon atom at the point of side chain substitution, transforming it from an sp^2 to an sp^3 carbon.

Using the Spartan 02 program (available from Wavefunction, Inc.), AM1[44−46] and AM1/SM5.4 (or SM5.4/A)[47] calculations were carried out on the same structures in order to evaluate the effect of solvent on the NCCN rotational barrier. The NCCN torsional angle between the two rings was allowed to vary between 0° and 180° in increments of 30°. Smaller increments and full optimization were used to locate nonplanar minima for only the tambjamine and enamine analogues. The AM1/SM5.4 solvation free energy was calculated at the AM1-optimized gas-phase geometry. Comparison of the ab initio and semiempirical results in vacuum followed by comparison of the AM1 and AM1/SM5.4 results provides a framework in which to link the vacuum phase ab initio results to the semiempirical solvation studies.

3. Results

The HF, DFT, and semiempirical results for the NCCN rotational barrier of the fragment molecules and tambjamine are given in Figures 2−5. In Figures 4 and 5, the E and Z relative energies for each case (ab initio, AM1, AM1/SM5.4) are calculated relative to whichever form (E or Z) has the GEM structure. Figure 5 also compares the HF and DFT results for neutral and protonated tambjamine in the E configuration. The same data are given in tabular form in the Supporting Information since the energy values of some of the minima are difficult to discern due to overlapping symbols in the figures. The results

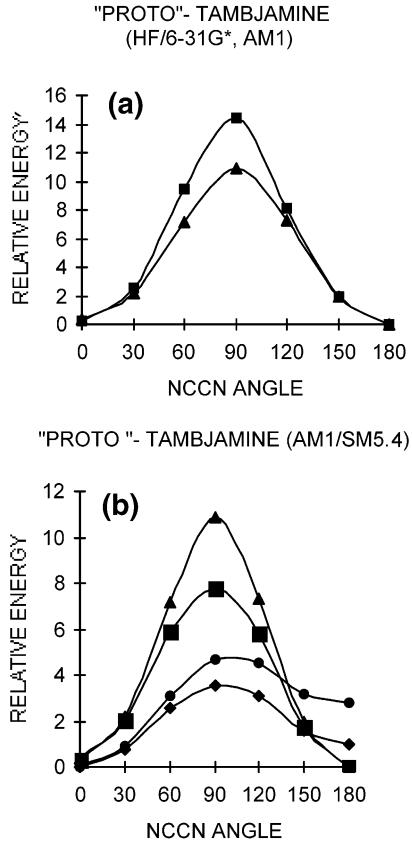

Figure 2. (a) NCCN rotational barrier for "proto"-tambjamine. Comparison of the HF/6-31G* and AM1 rotational barriers for the protonated molecule in vacuum phase. In this and subsequent figures, energy is given in kcal/mol and angle in degrees. Plot symbols: square−HF/6-31G*; triangle−AM1. (b) NCCN rotational barrier for "proto"-tambjamine. Comparison of the AM1 and AM1/SM5.4 rotational barriers for the neutral and protonated molecules in vacuum and solvent phase. Plot symbols: circle−neutral, vacuum, AM1; diamond−neutral, solvent, AM1/SM5.4; triangle−protonated, vacuum, AM1; square−protonated, solvent, AM1/SM5.4.

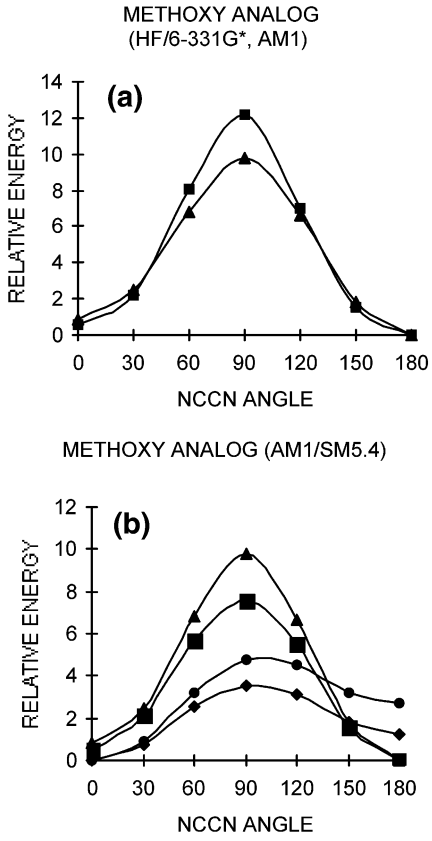

Figure 3. (a) NCCN rotational barrier for the methoxy analogue. Comparison of the HF/6-31G* and AM1 rotational barriers for the protonated molecule in vacuum phase. Plot symbols: square−HF/6-31G*; triangle−AM1. (b) NCCN rotational barrier for the methoxy analogue. Comparison of the AM1 and AM1/SM5.4 rotational barriers for the neutral and protonated molecules in vacuum and solvent phase. Plot symbols: circle−neutral, vacuum, AM1; diamond−neutral, solvent, AM1/SM5.4; triangle−protonated, vacuum, AM1; square−protonated, solvent, AM1/SM5.4.

are analyzed in terms of the various trends given in the subdivisions below.

A. Ability of AM1 to Reproduce HF/6-31G* Barrier Height and Minima in Vacuo. *Protonated Species.* For comparison of the HF/6-31G* and AM1 results for the protonated molecules in vacuum, see Figures 2a (proto-tambjamine), 3a (methoxy analog), 4a and 4b (enamine analog), and 5a and 5c (tambjamine). Figure 2a shows that the AM1 method reproduces the shape and location of the energy minimum (180°) and maximum (90°) of the HF/6-31G* curve for proto-tambjamine. The AM1 barrier (10.9 kcal/mol) is about 3.5 kcal/mol lower in energy than the ab initio barrier (14.4 kcal/mol). Similarly, Figure 3a shows that the AM1 method reproduces the shape and location of the energy minimum (180°) and maximum (90°) of the HF/6-31G* curve for the methoxy analogue. Here, the AM1 barrier (9.8 kcal/mol) is about 2.5 kcal/mol lower in energy than the ab initio barrier (12.2 kcal/mol). Figure 4a shows that the HF/6-31G* curves for the E and Z configurations of the enamine analogue are very similar, with the minimum occurring at ∠NCCN = 180° (0.8 and 0.0 kcal/mol, respectively). At ∠NCCN = 0° the energies are 2.7 and 2.5 kcal/mol, respectively. Figure 4b shows that the AM1 results for the E and Z configurations of the protonated enamine analogue are very similar to the HF/6-31G* results. In the case of tambjamine, the ab initio HF/6-31G* calculations (Figure 5a) indicate that both the E and Z configurations of tambjamine have a minimum at ∠NCCN = 166° (0.0 and 1.2 kcal/mol, respectively). A second minimum occurs around ∠NCCN = 20° (1.5 and 1.1 kcal/mol, respectively). Figure 5c shows that the AM1 results for the E and Z configurations of tambjamine are similar to the HF/6-31G* results, except that no nonplanar minima were found. This is in agreement with AM1 studies of a somewhat similar system, 2,2′-bipyrrole, which failed to reproduce the nonplanar local minima found by the MIDI-4 double-ζ basis set.[48]

Neutral Species. For comparison of the HF/6-31G* and AM1 results for neutral tambjamine in vacuum, see Figures 5b and 5d. Figure 5b shows that both the E and Z configurations of the neutral species in vacuum have the energy maximum occurring at 90° (10.3 and 8.5 kcal/mol, respectively). The Z configuration has a minimum at 0° (0.0 kcal/mol), while the E configuration has a minimum at 30° (3.6 kcal/mol). Figure 5d shows that the AM1 results for the E and Z configurations of the neutral species in vacuum are similar to the HF/6-31G* results, with the maximum occurring at 90° (4.8 and 4.2 kcal/mol, respectively). The Z configuration has a minimum at 0° (0.0 kcal/mol), as does the E configuration (0.5 kcal/mol).

In summary, the AM1 method qualitatively reproduces the shape and height of the HF/6-31G* NCCN torsional barriers of the protonated and neutral species in vacuum, with the height being underestimated by about 1−3.5 and 5 kcal/mol, respectively.

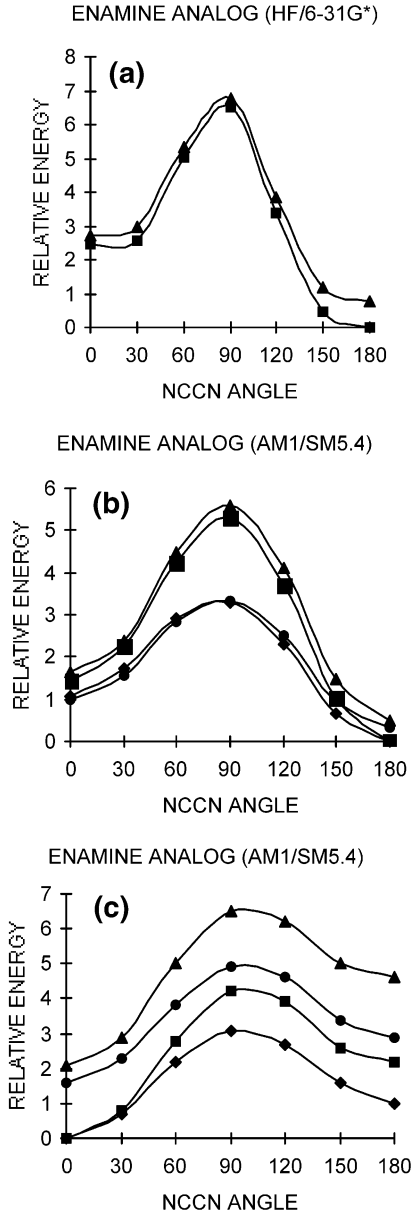

Figure 4. (a) NCCN rotational barrier for the enamine analogue. Comparison of the HF/6-31G* rotational barrier for the protonated E and Z configurations in vacuum phase. Plot symbols: square−Z; triangle−E. (b) NCCN rotational barrier for the enamine analogue. Comparison of the AM1 and AM1/SM5.4 rotational barriers for the protonated E and Z configurations in vacuum and solvent phase. Plot symbols: triangle−E, vacuum, AM1; circle−E, solvent, AM1/SM5.4; square−Z, vacuum, AM1; diamond−Z, solvent, AM1/SM5.4. (c) NCCN rotational barrier for the enamine analogue. Comparison of the AM1 and AM1/SM5.4 rotational barriers for the neutral E and Z configurations in vacuum and solvent phase. Plot symbols: triangle−E, vacuum, AM1; circle−E, solvent, AM1/SM5.4; square−Z, vacuum, AM1; diamond−Z, solvent, AM1/SM5.4.

B. Effect of Side Chains on NCCN Rotational Barrier of Protonated Species in Vacuo. Comparing the ab initio results in Figures 2a and 3a shows that addition of the methoxy substituent to the B ring has little effect on the magnitude of the NCCN torsional barrier. The HF/6-31G* barrier is 14.4 kcal/mol for proto-tambjamine and 12.2 kcal/mol for the methoxy analogue. Figure 4a shows that addition of the enamine side chain to the proto-tambjamine template has a much more pronounced effect, reducing the barrier to 6.8 and 6.5 kcal/mol for the E and Z configurations, respectively. Comparing Figures 5a to 4a shows that addition of the methoxy group to the

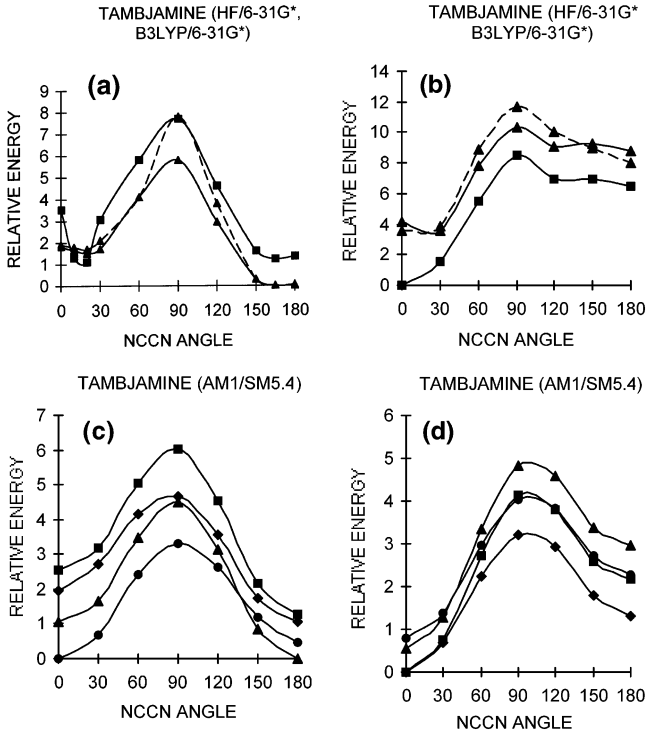

Figure 5. (a) NCCN rotational barrier for tambjamine. Comparison of the HF/6-31G* rotational barrier for the protonated E and Z configurations to the B3LYP/6-31G* rotational barrier for the protonated E configuration in vacuum phase. Plot symbols: square−Z; triangle−E, solid line−HF/6-31G*; dotted line−B3LYP/6-31G*. (b) NCCN rotational barrier for tambjamine. Comparison of the HF/6-31G* rotational barrier for the neutral E and Z configurations to the B3LYP/6-31G* rotational barrier for the neutral E configuration in vacuum phase. Plot symbols: square−Z; triangle−E, solid line−HF/6-31G*; dotted line−B3LYP/6-31G*. (c) NCCN rotational barrier for tambjamine. Comparison of the AM1 and AM1/SM5.4 rotational barriers for the protonated E and Z configurations in vacuum and solvent phase. Plot symbols: triangle−E, vacuum, AM1; circle−E, solvent, AM1/SM5.4; square−Z, vacuum, AM1; diamond−Z, solvent, AM1/SM5.4. (d) NCCN rotational barrier for tambjamine. Comparison of the AM1 and AM1/SM5.4 rotational barriers for the neutral E and Z configurations in vacuum and solvent phase. Plot symbols: triangle−E, vacuum, AM1; circle−E, solvent, AM1/SM5.4; square−Z, vacuum, AM1; diamond−Z, solvent, AM1/SM5.4.

enamine analogue to form tambjamine reduces the barrier from 14.4 kcal/mol for proto-tambjamine to 5.8 and 7.7 kcal/mol for the E and Z configurations, respectively. As in the protonated case, the AM1 results qualitatively reproduce the HF/6-31G* results. In summary, the enamine side chain has a much larger effect than the methoxy side chain on lowering the NCCN rotational barrier.

C. Effect of Protonation on NCCN Rotational Barrier in Vacuo. For tambjamine, comparison of the HF/6-31G* results in Figures 5a (protonated) and 5b (neutral) shows that the barrier height is larger in the neutral than the protonated case but that the magnitude of the protonation effect depends on whether the molecule is in the E or Z configuration. This difference is considerable: 4.5 kcal/mol for the neutral versus protonated E configuration barriers compared to 0.8 kcal/mol for the neutral versus protonated Z configuration barriers. The AM1 results (Figures 5c and 5d) repeat the trends of the ab initio results for the E configuration. The NCCN barrier for the neutral E configuration is 0.3 kcal/mol higher than that of the protonated E configuration, but the barrier for the neutral Z configuration is 1.9 kcal/mol lower than that of the protonated Z configuration.

In summary, in going from the simple systems (proto-

TABLE 1: Tambjamine H···H Distances[a] (Å) for Planar Conformers, HF/6-31G* and B3LYP/6-31G* Methods[b]

tambjamine[c]	∠NCCN = 0° CH(A)···CH(B)	∠NCCN = 180° NH(A)···CH(B)	∠NCCN = 0° NH(A)···NH(B)	∠NCCN = 180° CH(A)···NH(B)
E − CAT (V)	2.501 (2.514)	2.410 (2.434)	2.328 (2.364)	2.409 (2.428)
Z − CAT (V)	2.492	2.404	2.317	2.392
E − NEU (V)	2.674 (2.733)	2.348 (2.361)		
Z − NEU (V)	2.656	2.342		

[a] NH(A) is the hydrogen on the A-ring nitrogen, NH(B) is the hydrogen on the B-ring nitrogen, and CH(A) and CH(B) are the hydrogens from the two rings which come into closest contact during the NCCN rotation. [b] B3LYP/6-31G* results in parentheses. [c] E−CAT(V): E configuration, protonated molecule, vacuum phase; Z−CAT(V): Z configuration, protonated molecule, vacuum phase; E−NEU(V): E configuration, neutral molecule, vacuum phase; Z−NEU(V): Z configuration, neutral molecule, vacuum phase.

tambjamine and the methoxy analog) to tambjamine, the relationship between the NCCN barrier in the protonated versus the neutral species becomes, in tambjamine, dependent on whether the molecule is in the E or Z configuration. For the simple systems (Figures 2b and 3b), the barrier is higher for the protonated species compared to the neutral species. For tambjamine (Figures 5c and 5d), this relationship depends on whether the molecule is in the E or Z configuration.

D. Effect of Electron Correlation on the NCCN Rotational Barrier in Vacuo. Figures 5a and 5b compare the NCCN rotational barrier calculated by the B3LYP/6-31G* method to the HF/6-31G* barrier for the E configuration of protonated and neutral tambjamine, respectively. The curves exhibit similar behavior, with the DFT barrier being about 2.0 kcal/mol higher than the HF barrier for both the neutral and protonated species. The B3LYP/6-31G*(d,p) results (not shown) were almost the same as the B3LYP/6-31G* results.

E. Relative Stability of ∠NCCN = 0° versus ∠NCCN = 180° Conformers. For both the E and Z configurations of protonated tambjamine (Figure 5a), the conformer at ∠NCCN = 180° is lower in energy than that at ∠NCCN = 0°. Poor steric interactions between the hydrogens in the planar conformers affect the relative energies of the ∠NCCN = 0° and 180° conformers. The H···H distances of closest approach during NCCN rotation are found for the planar conformers and are listed in Table 1. The table shows that the H···H distances calculated by the B3LYP/6-31G* method for the planar conformations are not significantly different from the HF/6-31G* results. Table 1 shows that for both the protonated E and Z configurations, the closest H···H distance is NH(A) ···NH-(B) at ∠NCCN = 0°, making this conformer slightly less stable than that at ∠NCCN = 180°. For both the E and Z configurations of neutral tambjamine (Figure 5b), the ∠NCCN = 0° conformer is of lower energy than the ∠NCCN = 180° conformer. Since there is no NH(B) proton, the NH(A) hydrogen interacts favorably with the lone pair on the B-ring nitrogen, stabilizing the ∠NCCN = 0° conformer. In addition, the closest H··H distance is NH(A)···CH(B) at ∠NCCN = 180° (Table 1), which contributes to making this conformer less stable than that at ∠NCCN = 0°.

F. Nonplanarity of the Tambjamine Rings. For both the E and Z configurations of protonated tambjamine (Figure 5a), the HF/6-31G* GEM conformer occurs at a nonplanar value (∠NCCN = 165−166°) and there is another local minimum at about ∠NCCN = 20°. Poor steric interactions between the hydrogens in the planar conformers (Table 1) result in the preference for nonplanar conformers. The B3LYP/6-31G* method found a local minimum of the protonated E configuration at ∠NCCN = 16° and, in contrast to the HF result, found the GEM conformer to be planar (∠NCCN = 180°). The MP2/6-31G* method was used for comparison purposes and located the GEM structure for the protonated E configuration at ∠NCCN = 154° with a local minimum at 28°. For neutral tambjamine (Figure 5b), no attempt was made to use full optimization to exactly locate the minima with the HF, DFT, or MP2 methods. For the E configuration, the HF/6-31G* method found the GEM conformer to be around ∠NCCN = 30° and a local minimum around 120°. The B3LYP/6-31G* method found the GEM conformer to be around ∠NCCN = 0° and a local minimum at 180°.

TABLE 2: Inter-ring C−C Bond Lengths (Å), HF/6-31G* and B3LYP/6-31G* methods,[a] Vacuum Phase

analogue[b]	NCCN = 0°	NCCN = 90°	NCCN = 180°
proto-tambjamine (CAT)	1.404	1.471	1.406
methoxy (CAT)	1.413	1.472	1.414
enamine (E, CAT)	1.434	1.471	1.436
tambjamine (E, CAT)	1.436 (1.436)	1.472 (1.472)	1.438 (1.438)
enamine (Z, CAT)	1.432	1.471	1.434
tambjamine (Z, CAT)	1.434	1.472	1.436
tambjamine (E, NEU)	1.459 (1.459)	1.481 (1.481)	1.462 (1.462)
tambjamine (Z, NEU)	1.458	1.481	1.461

[a] B3LYP/6-31G* in parentheses. [b] CAT: protonated molecule; E, CAT: protonated molecule in E configuration; Z, CAT: protonated molecule in Z configuration; E, NEU: neutral molecule in E configuration; Z, NEU: neutral molecule in Z configuration.

G. Degree of π Delocalization of the Tambjamine Rings. Table 2 summarizes the inter-ring C−C distances for the various analogues. In all the systems, a small increase in the inter-ring C−C bond length is noted upon going from the planar to the perpendicular conformation. Such bond lengths are more typical of a $C(sp^2)-C(sp^2)$ bond than a truly aromatic system and correspond to a small amount of π delocalization between the rings.[49] The DFT and HF results for tambjamine are identical.

H. Effect of Solvent on the NCCN Rotational Barrier of Protonated and Neutral Species. The AM1/SM5.4 results for proto-tambjamine (Figure 2b) and the methoxy analogue (Figure 3b) are very similar and show that the effect of solvent is to significantly lower the barrier (by about 2−3 kcal/mol) for the protonated species and to lower it by a smaller amount (about 1 kcal/mol) for the neutral species. Likewise, for the enamine analogue, Figure 4b shows that the effect of solvation is to lower the NCCN rotational barrier of the protonated species by about 2 kcal/mol for both the E and Z configurations. Figure 4c shows a lesser effect in the neutral case (about 1−1.6 kcal/mol for both configurations). Figures 5c and 5d show the effect of solvent on the NCCN barrier for the protonated and neutral species of tambjamine, respectively. Figure 5c shows that the effect of solvation is to lower the NCCN rotational barrier by about 1.3 kcal/mol for both the E and Z configurations of the protonated species. Since for the enamine analogue this drop is somewhat larger, the effect of the methoxy substituent in protonated tambjamine is to modulate the solvent lowering of the NCCN rotational barrier seen in the protonated enamine analogue. Figures 4c and 5d show that the effect of solvation is less for the enamine and tambjamine neutral analogues.

In summary, the effect of solvent is to decrease the NCCN rotational barrier of the protonated species and to cause less of

a decrease for the neutral species. The decrease in the NCCN rotational barrier of the protonated species in solvent becomes smaller as side chains are added to the proto-tambjamine template to form tambjamine.

I. Stability of E versus Z Configurations. *Enamine Analogue.* The HF/6-31G* results for the protonated species in vacuum phase (Figure 4a) show that the Z configuration is consistently close in energy to and more stable than the E for all values of NCCN. This trend is repeated in the AM1 results (Figure 4b). The AM1 solvent phase results indicate that the E and Z configurations are extremely close in energy. Figure 4c shows that for the neutral species the Z is more stable than E in both vacuum and solvent.

Tambjamine. The HF/6-31G* results for the protonated species in vacuum phase (Figure 5a) show that the E configuration is consistently lower in energy than the Z except in a small region ($\angle$NCCN = 10−20°). This general trend (E < Z) is repeated in the AM1 results in both vacuum and solvent (Figure 5c). Comparison of Figure 5b to Figures 5a and 5d shows that this trend is reversed in the HF/6-31G*, AM1, and AM1/SM5.4 results for the neutral analogue.

In summary, all the methods (HF/6-31G*, AM1, AM1/SM5.4) show that the Z configuration of the neutral species of the enamine analogue and tambjamine is more stable than the E (except for the AM1/SM5.4 results for the enamine analog). For the biologically active species, protonated tambjamine, all the methods reverse this trend.

4. Discussion

Tambjamine is an unfused aromatic bicyclic system, which in its protonated form intercalates into DNA with a preference for AT sites. The present quantum mechanical study was undertaken in order to investigate the effect of the protonation, side chains, solvent, and electron correlation on the NCCN rotational barrier, as well as to determine the degree of relative planarity of the A and B rings. These properties relate to the flexibility of tambjamine and give an indication of the energetic cost involved in adjusting its inter-ring twist angle to adopt the propeller twist of DNA in order to form a nonclassical intercalation complex. The E configuration of protonated tambjamine was found to be more stable than the Z configuration due to solvent stabilization and the formation of a pseudo six-membered ring by intramolecular hydrogen bonding. Inclusion of electron correlation increased the NCCN rotational barrier by about 2 kcal/mol. Solvent and the presence of the enamine side chain were shown to have a significant effect in lowering the NCCN rotational barrier. For protonated tambjamine both the HF and DFT methods predicted nonplanar minima around 20°, whereas DFT calculated the GEM to be planar (180°) in contrast to the HF nonplanar GEM (166°). However, both the HF and DFT results showed that there are broad regions ($\angle$NCCN = 0−30° and 150−180°) with a minimal energetic cost for the E configuration of protonated tambjamine to adopt a nonplanar conformation. Therefore, both methods predict that the molecule has significant flexibility in adjusting its conformation to the propeller twist of the DNA binding site in order to form a nonclassical intercalation complex. These issues are discussed in detail below.

A. Comparison of Tambjamine HF and DFT Results to 2,2′-Bipyrrole. The 2,2′-bipyrrole system[50,51] is somewhat similar to the protonated molecules studied here. Note that proto-tambjamine is not exactly the same molecule as 2,2′-bipyrrole because of the sp^3 carbon in the B ring of proto-tambjamine. Since, in the present work, the existence of nonplanar conformations was explored only for protonated tambjamine (rather than the analogues), only those results are compared below.

Millefiori and Alparone[49] studied the rotational barrier between the A and B rings in 2,2′-bipyrrole using the HF/6-31G*, MP2/6-31G*, and B3LYP/6-31G* basis sets. They found the B3LYP results to be consistently higher, and the MP2 results to be consistently lower, than the HF results. In the perpendicular conformation, the B3LYP energy was 0.95 kcal/mol higher, and the MP2 energy was 1.37 kcal/mol lower, than the HF energy. They attributed this to the tendency of the DFT method to favor π-electron contributions (thus stabilizing planar conformers) in contrast to the MP2 method, which emphasizes nonbonded interactions (and favors twisted conformers). They found the molecule to be nonplanar with its GEM conformer the anti-gauche ($\angle$NCCN = 145.8°, 138.2°, and 150.0° in the HF, MP2, and B3LYP calculations, respectively). Another local minimum was identified as the syn-gauche conformer with $\angle$NCCN = 42.5° (1.53 kcal/mol), 45.7° (0.16 kcal/mol), and 40.3° (2.48 kcal/mol) in the HF, MP2, and B3LYP calculations, respectively. The barrier height was 1.53 kcal/mol (NCCN = 81.1°, HF), 0.16 kcal/mol ($\angle$NCCN =73.8°, MP2), and 2.48 kcal/mol ($\angle$NCCN = 82.3°, B3LYP). They noted the variation in the inter-ring C−C bond with NCCN torsional angle. From the anti ($\angle$NCCN = 180°) values of 1.458, 1.447, and 1.448 Å, the C−C bond length increased to 1.472, 1.458, and 1.466 Å in the perpendicular conformation for the HF, MP2, and B3LYP calculations, respectively. These increases are small and indicate that there is only a small amount of π delocalization between the rings.

Karpfen et al.[52] used the HF/6-31G(d), MP2/6-31G(d), and B3LYP/6-31G(d) basis sets to study torsional barriers in 2,2′-bipyrrole and five other molecules with varying degrees of conjugation: 1,3-butadiene, styrene, biphenyl, 2,2′-bithiophene, and 2,2′-bifuran. Except for 2,2′-bifuran, they found the B3LYP method to give consistently higher (and the MP2 results to be consistently lower) energies than the HF method. They found the HF barriers to be closer to experimental results (where available). Except for 2,2′-bifuran, the DFT energy was found to be 1−2.5 kcal/mol higher than the HF energy for the perpendicular conformation of the molecules. The DFT method generally predicted shallower minima that were notably offset in torsional angle value from the HF and MP2 minima. For styrene, the DFT method predicted planar, while the HF and MP2 methods predicted nonplanar, minima. Extension to the 6-311++G (d,p) basis set had little effect on the NCCN barrier. This is consistent with studies on biphenyl in which increasing the basis set size in DFT calculations had only a small effect on the energy.[53]

The tambjamine HF/6-31G* results are consistent with the above findings in identifying nonplanar conformations as local minima on the NCCN potential energy surface. For protonated tambjamine the GEM structure was found at 166° and another local minimum around 20° for both the E and Z configurations. The tambjamine DFT results are also consistent with the above findings in that the DFT energy was found to be about 2 kcal/mol higher than the HF results for the perpendicular conformation. As above, increasing the basis set size from 6-31G* to 6-31G*(d,p) in the B3LYP calculation had an insignificant effect on the rotational barrier. In addition, the DFT method predicted planar (180°) minima for protonated tambjamine, in contrast to the HF result (166°). Both methods predicted a nonplanar minimum around 20° (HF: 20°, DFT: 16°). This is consistent with the tendency of the DFT method, as noted in the above studies,[49,52] to predict shallower minima and higher rotational

barriers than the HF method. This is probably due to the "overdelocalization" problem of DFT.[54]

Similar to 2,2′-bipyrrole, the tambjamine systems studied here exhibit a small degree of π delocalization between the rings. The same small increase in the inter-ring C−C bond length as with 2,2′-bipyrrole was noted for tambjamine in both the HF and DFT calculations upon going from the planar to the perpendicular conformation. In summary, the trends noted in the HF/6-31G* and B3LYP/6-31G* tambjamine results are qualitatively similar to those found for a similar system, such as 2,2′-bipyrrole.

B. E versus Z Stability of Tambjamine. The ab initio and semiempirical results in vacuum and solvent show that the E configuration of tambjamine is more stable than the Z for the protonated case (Figures 5a and 5c), while the reverse is true in the neutral case (Figures 5b and 5d). For the enamine analogue, the Z configuration is more stable than the E for both the neutral and protonated species in vacuum (Figures 4a, 4b, and 4c). These results indicate that only with the addition of the methoxy group to the enamine cation to form the tambjamine cation is the E configuration stabilized with respect to the Z. In the E configuration, a pseudo six-membered ring is formed by hydrogen bonding between the amino hydrogen of the enamine group and the oxygen of the methoxy group, stabilizing the E configuration relative to the Z. Significantly, both the HF/6-31G* and B3LYP/6-31G* results show that throughout the NCCN rotation, the amino hydrogen−methoxy oxygen distance is maintained at 2.2 Å, indicating that the inclusion of electron correlation has little effect on the formation of this hydrogen bond. In the Z configuration, however, a repulsive interaction is formed by the proton on the B-ring nitrogen and the amino hydrogen on the enamine group, which may contribute to the lower stability of this conformer. The HF/6-31G* results show that throughout the NCCN rotation, the proton-amino hydrogen distance is maintained at 2.4 Å. In neutral tambjamine, the Z configuration is more stable than the E because, in the absence of the proton, the amino hydrogen on the enamine group is allowed to form an attractive interaction with the lone pair of the B-ring nitrogen. The HF/6-31G* results show that throughout the NCCN rotation, the B-ring nitrogen-amino hydrogen distance is 2.5 Å.

The AM1 and AM1/SM5.4 results can be combined in the following thermodynamic cycle to obtain the free energy of solvation for neutral and protonated tambjamine

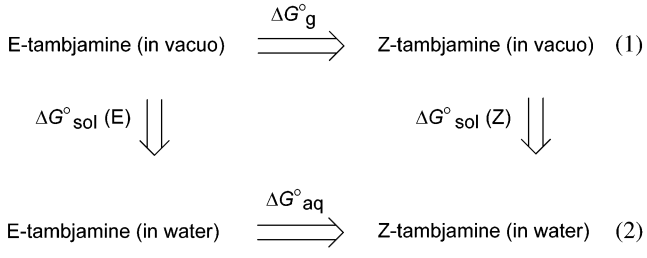

where ΔG°_{aq}, the free energy of solvation, can be approximated by

$$\Delta G^\circ_{aq} = \Delta G^\circ_g + \Delta G^\circ_{sol}(Z) - \Delta G^\circ_{sol}(E)$$

and ΔG°_{sol} is approximated in the AM1/SM5.4 method as the enthalpy of the E or Z configuration in water minus that in vacuo.

Also,

$$\Delta G^\circ_g = E_{EN}(Z,g) - E_{EN}(E,g)$$

TABLE 3: AM1/SM5.4 Energies (kcal/mol) for Thermodynamic Cycle Calculation

tambjamine	ΔG°_g	ΔG°_{sol} (E)	ΔG°_{sol} (Z)	ΔG°_{aq}
neutral	−0.56	−10.51	−10.75	−0.80
protonated	1.27	−41.95	−42.19	1.03

where E_{EN} is the gas-phase electronic and nuclear Coulombic energy of the E or Z configurations.

The AM1 GEM conformers of the E and Z configurations were used in the calculations. Table 3 gives the individual contributions to the free energy of solvation, which was found to be equal to −0.80 and 1.03 kcal/mol for neutral and protonated tambjamine, respectively. This means that, for the neutral case, eq 2 is spontaneous as written and the Z configuration is the more stable. The opposite is true for the protonated species. These results are consistent with the relative energy profiles shown in Figure 5. In summary, both the vacuum- and solvent-phase calculations show that the E configuration of protonated tambjamine is more stable than the Z.

C. Solvent Models. The SM5.4 model is only one of several self-consistent reaction field (SCRF) continuum solvent models[55] that could have been used to estimate the effect of aqueous media on the NCCN rotational barrier of tambjamine. The total solvation free energy is a sum of the long-range electrostatic contribution and short-range terms, such as cavitation, dispersion, exchange-repulsion interactions between solvent and solute, and changes due to perturbation of solvent structure. Curutchet et al.[56] systematically compared the free energy of solvation of 18 small polar, neutral molecules using the HF/6-31G(d) basis set and the SM5.42R model,[57] the multipolar expansion model (MPE),[58] and the polarizable continuum model (PCM).[59] The solute cavity, permittivity of the medium, and representation of the charge density were varied in the same way for each model. The SM5.42R model is similar to the AM1/SM5.4 (or SM5.4/A) model employed in the present study. Both are variations of Solvation Model 5[47] with class IV atomic charges.[60] SM5.4R uses charge model 2 (CM2)[61] atomic charges; SM5.4A, charge model 1 (CM1).[60] In both the present paper and in the work of Curutchet et al., the solvation free energy was calculated for a given rigid gas-phase geometry, as the structure was not allowed to relax in the solvent. Although the SM5.42R model calculated electrostatic free energies that were smaller in magnitude than those of the other two methods (when identical cavities were employed), all three SCRF methods gave total solvation free energies in agreement with each other and with experiment. Since a full-scale comparison of SCRF solvent models for tambjamine is beyond the scope of the present work, it will be the subject of a future publication.

D. Effect of B-Ring Substitution and Protonation on the NCCN Rotational Barrier. Melvin et al.[21] have shown that a neutral aldehyde precursor of tambjamine, which contains the methoxy substituent but with an aldehyde group replacing the enamine side chain, does not bind to DNA. This indicates that both the enamine side chain and a positive charge are important for DNA binding. The calculations suggest a reason for this finding. The ab initio results show that the NCCN rotational barrier for the protonated species dramatically drops as the substituents are added, the most significant drop occurring when the enamine side chain is added. The barrier for prototambjamine is the highest at 14.5 kcal/mol, dropping to 12.2 kcal/mol in the methoxy analogue, to 6.5 kcal/mol in the enamine system, and finally to 5.8 kcal/mol for the E configuration of tambjamine. This shows the importance of the enamine side chain. Similarly the calculations show that for

TABLE 4: Propeller Twist Values from BDL084.pdb

base pair	base pair type	propeller twist (degrees)
1	C−G	−17.31
2	G−C	−14.30
3	C−G	−5.40
4	G−C	−9.45
5	A−T	−15.31
6	A−T	−15.00
7	T−A	−16.74
8	T−A	−16.36
9	C−G	−10.27
10	G−C	−9.60
11	C−G	−17.42
12	G−C	−4.95

proto-tambjamine the barrier for the protonated species is higher than that for the neutral species, but that this trend is reversed in tambjamine. This lowering of the NCCN rotational barrier in protonated tambjamine has a significant effect on the flexibility of the molecule−a factor that may be crucial for the ability of tambjamine to intercalate between the DNA base pairs.

As a further proof of this point, the AM1/SM5.4 results predict a drop in the barrier height for all the systems, whether neutral or protonated. In fact, in the protonated E configurations of the enamine analogue (Figure 4b) and tambjamine (Figure 5c), the barrier to rotation is so low that there is essentially free rotation (3.3 kcal/mol in both cases). Again, this may indicate that the "bioactive" or binding conformation for DNA intercalation can be easily achieved by protonated tambjamine since the A ring can rotate to any position needed for optimum biological interaction.

E. DNA Binding of Unfused Aromatic Cations. Tambjamine and amiloride are unfused aromatic cations that are AT-specific intercalators. The HF and DFT results for the E configuration of protonated tambjamine in vacuum (Figure 5a) show that there is a wide range of NCCN values (0−30° and 150−180°) for which the energy "cost" of the molecule, assuming a nonplanar conformation, is minimal. The same behavior was noted for amiloride.[28] Similarly, Figure 5c shows that in the presence of solvent the energy cost of the protonated E form of tambjamine attaining a nonplanar conformer is minimal in the ranges ∠NCCN = 0−30° or 150−180°. This indicates that the molecule has a great deal of flexibility in adjusting its conformation to the DNA binding site.

As mentioned in the Introduction, many unfused polyaromatic cations form a nonclassical intercalation complex in which the inter-ring twist angle of the molecule as well as the propeller twist of DNA are unchanged upon complexation.[13,15,16,17] So the wide range of NCCN values for which the E configuration of protonated tambjamine has low energy values may be an important factor in allowing the ligand to adjust its inter-ring orientation to the DNA propeller twist.

The 3DNA program (http://rutchem.rutgers.edu/~xiangjun/3DNA/index.html),[62] available through the Rutgers Nucleic Acid Database (NDB; http://ndbserver.rutgers.edu/NDB/),[63,64] can be used to determine the base pair and base step parameters for X-ray structures of DNA. An example given on the 3DNA website is the structure of the B-DNA dodecamer 5′-d(CpG-pCpGpApApTpTpCpGpCpG)-3′ (Nucleic Acid Database ID: BDL084).[65] The values of the propeller twist for each of the base pairs in the dodecamer are reproduced in Table 4.

In this example, the A−T and T−A base pairs have a propeller twist angle of 15−17°. The G−C and C−G propeller twist values range from about 5−17°. Olson et al.[66] used 3DNA and seven other software packages to calculate with respect to a standard reference frame the local helical parameters of 31 A-DNA and 22 B-DNA structures from the NDB. They found the values of the parameters to be independent of calculation method. The mean values of propeller twist averaged over A−T, T−A, G−C, and C−G base pairs (with standard deviation given in parentheses) are −11.8° (4.1) and −11.4° (5.3) for A- and B-DNA, respectively.

The quantum mechanical results reported here find tambjamine to have two nonplanar low energy conformers and a wide range of NCCN angles for which the conformational energy is low. This indicates that the flexibility of tambjamine around the inter-ring bond could allow the molecule to adjust its NCCN angle to fit the propeller twist of the base pair upon intercalation. Since the A−T and T−A base pairs have propeller twist angles similar to those of the C−G and G−C base pairs, this does not explain why tambjamine is an AT specific intercalator. The answer may lie in a subtle interplay of stacking, electrostatic, and steric interactions. Future work will involve quantum mechanical studies of the stacking of tambjamine with A−T versus C−G base pairs and NMR and molecular dynamics studies of tambjamine/DNA complexes.

Acknowledgment. C.A.V. thanks the donors of the Petroleum Research Fund, Grant 36982-B4, administered by the American Chemical Society, for partial support of this research.

Supporting Information Available: The material consists of tables corresponding to Figures 2−5. This material is available free of charge via the Internet at http://pubs.acs.org.

References and Notes

(1) Wada, K.; Mizutani, T.; Matsuoka, H.; Kitagawa, S. *Chem. Eur. J.* **2003**, *9*, 2368.
(2) Denny, W. A. *Anti-Cancer Drug Des.* **1989**, *4*, 241.
(3) Neidle, S. Computer Modelling of Drug-DNA Intercalative Interactions. In *The Design of Drugs to Macromolecular Targets*; Beddell, C. R., Ed.; John Wiley & Sons: Chichester, New York, 1992.
(4) Wang, A. H.-J. *Cur. Opin. Struct. Biol.* **1992**, *2*, 361.
(5) Waring, M. J.; Bailly, C. *J. Mol. Recog.* **1994**, *7*, 109.
(6) Trent, J. O.; Neidle, S. Molecular Modeling of Drug-DNA Interactions: Facts and Fantasies. In *Advances in DNA Sequence Specific Agents*; Hurley, L., Ed.; JAI Press: Greenwich, CT, 1996; Vol. 2, pp 29−58.
(7) Nguyen, B.; Tardy, C.; Colson, P.; Houssier, C.; Kumar, A.; Boykin, D. W.; Wilson, W. D. *Biopolymers* **2002**, *63*, 281.
(8) Bailly, C.; Hénichart, J.-P.; Colson, P.; Houssier, C. *J. Mol. Recog.* **1992**, *5*, 155.
(9) Bailly, C.; Cuthbert, A. W.; Gentle, D.; Knowles, M. R.; Waring, M. J. *Biochem.* **1993**, *32*, 2514.
(10) Sarma, M. H.; Mitra, C. K.; Sarma, R. H. *Int. J. Quantum Chem. Quantum Biol. Symp.* **1980**, *7*, 1.
(11) Bailly, C.; Waring, M. J. *Biochem.* **1993**, *32*, 5985.
(12) Wilson, W. D.; Wang, Y.-H.; Kusuma, S.; Chandrasekaran, S.; Yang, N. C.; Boykin, D. W. *J. Am. Chem. Soc.* **1985**, *107*, 4989.
(13) Wilson, W. D.; Strekowski, L.; Tanious, F. A.; Watson, R. A.; Morosz, J. L.; Strekowska, A.; Webster, G. D.; Neidle, S. *J. Am. Chem. Soc.* **1988**, *110*, 8292.
(14) Strekowski, L.; Mokrosz, J. L.; Tanious, F. A.; Watson, R. A.; Harden, D. B.; Mokrosz, M. J.; Edwards, W. D.; Wilson, W. D. *J. Med. Chem.* **1988**, *31*, 1231.
(15) Wilson, W. D.; Tanious, F. A.; Watson, R. A.; Barton, H. J.; Strekowska, A.; Harden, D. B.; Strekowski, L. *Biochem.* **1989**, *28*, 1984.
(16) Strekowski, L.; Mokrosz, J. L.; Wilson, W. D.; Mokrosz, M. J.; Stretkowski, A. *Biochem.* **1992**, *31*, 10802.
(17) Wilson, W. D.; Tanious, F. A.; Barton, H. J.; Wydra, R. L.; Jones, R. L.; Boykin, D. W.; Strekowski, L. *Anti-Cancer Drug Des.* **1990**, *5*, 31.
(18) Wilson, W. D.; Tanious, F. A.; Buczak, H.; Venkatramanan, M. K.; Das, B. P.; Boykin, D. W. *Jerusalem Symp. Quantum Chem. Biochem.* **1990**, *23*, 331.
(19) Wilson, W. D.; Barton, H. J.; Tanious, F. A.; Kong, S.-B.; Strekowski, L. *Biophys. Chem.* **1990**, *35*, 227.
(20) Wilson, W. D.; Tanious, F. A.; Ding, D.; Kumar, A.; Boykin, D. W.; Colson, P.; Houssier, C.; Bailly, C. *J. Am. Chem. Soc.* **1998**, *120*, 10310.
(21) Melvin, M. S.; Ferguson, D. C.; Lindquist, N.; Manderville, R. A. *J. Org. Chem.* **1999**, *64*, 6861.

(22) Becker, H.-C.; Norden, B. *J. Am. Chem. Soc.* **1999**, *121*, 11947.
(23) Benos, D. J. Amiloride: Chemistry, Kinetics, and Structure−Activity Relationships. In *Na^+/H^+ Exchange*; Grinstein, S., Ed.; CRC: Boca Raton, 1988; pp 121−136.
(24) Garty, H.; Benos, D. J. *Physiol. Rev.* **1988**, *68*, 309.
(25) Kleyman, T. R.; Cragoe, E. J., Jr. *J. Membr. Biol.* **1988**, *105*, 1.
(26) *Cation Transport Probes: The Amiloride Series*; Kleyman, T. R.; Cragoe, E. J., Jr., Eds.; Academic: New York, 1990; Vol. 191, pp 739−755.
(27) Venanzi, C. A.; Plant, C.; Venanzi, T. J. *J. Comput. Chem.* **1991**, *12*, 850.
(28) Buono, R. A.; Venanzi, T. J.; Zauhar, R. J.; Luzhkov, V. B.; Venanzi, C. A. *J. Am. Chem. Soc.* **1994**, *116*, 1502.
(29) Venanzi, C. A.; Buono, R. A.; Skawinski, W. J.; Busanic, T. J.; Venanzi, T. J.; Zauhar, R. J.; Luzhkov, V. B. From Maps to Models: A Concerted Computational Approach to Analysis of the Structure−Activity Relationships of Amiloride Analogues. In *Computer-Aided Molecular Design: Applications in Agrochemicals, Materials, and Pharmaceuticals*; Reynolds, C. H., Holloway, M. K., Cox, H. K., Eds.; ACS Symposium Series 589, American Chemical Society: Washington, DC, 1995; pp 51−63.
(30) Venanzi, C. A.; Plant, C.; Venanzi, T. J. *J. Med. Chem.* **1992**, *35*, 1643.
(31) Venanzi, C. A.; Venanzi, T. J. Molecular Modeling Studies of Amiloride Analogs. In *Mechanisms of Taste Transduction*; Simon, S. A., Roper, S. D., Eds.; CRC: Boca Raton, 1993; pp 428−462.
(32) Venanzi, C. A.; Buono, R. A.; Luzhkov, V. B.; Zauhar, R. J.; Venanzi, T. J. Case Studies in Solvation of Bioactive Molecules: Amiloride, a Sodium Channel Blocker; β-Cyclodextrin, an Enzyme Mimic. In *Structure and Reactivity in Aqueous Solution: Characterization of Chemical and Biological Systems*; Cramer, C. J., Truhlar, D. G., Eds.; ACS Symposium Series 568, American Chemical Society: Washington, D.C., 1994; pp 260−279.
(33) Li, J. H.-Y.; Cragoe, E. J., Jr.; Lindemann, B. *J. Membr. Biol.* **1985**, *83*, 45.
(34) Li, J. H.-Y.; Cragoe, E. J., Jr.; Lindemann, B. *J. Membr. Biol.* **1987**, *95*, 171.
(35) Besterman, J. M.; Elwell, L. P.; Blanchard, S. G.; Cory, M. *J. Biol. Chem.* **1987**, *262*, 13352.
(36) Ofsievich, A. D.; Skawinski, W. J.; Buono, R. A.; Venanzi, C. A. *Struct. Chem.* **2002**, *13*, 73.
(37) Bondarev, D. B.; Skawinski, W. J.; Venanzi, C. A. *J. Phys. Chem.* **2000**, *104*, 815.
(38) Monaco, R. R.; Polkosnik, W. *J. Biomol. Str. Dyn.* **1996**, *14*, 13.
(39) Monaco, R. R.; Polkosnik, W.; Dwarakanath, S. *J. Biomol. Struct. Dyn.* **1997**, *15*, 63.
(40) Elcock, A. H.; Rodger, A.; Richards, W. G. *Biopolymers* **1996**, *39*, 309.
(41) Frisch, M. J.; Trucks, G. W.; Schlegel, H. B.; Scuseria, G. E.; Robb, M. A.; Cheeseman, J. R.; Zakrzewski, V. G.; Montgomery, J., J. A.; Stratmann, R. E.; Burant, J. C.; Dapprich, S.; Millam, J. M.; Daniels, A. D.; Kudin, K. N.; Strain, M. C.; Farkas, O.; Tomasi, J.; Barone, V.; Cossi, M.; Cammi, R.; Menucci, B.; Pomelli, C.; Adamo, C.; Clifford, S.; Ochterski, J.; Petersson, G. A.; Ayala, P. Y.; Cui, Q.; Morokuma, K.; Rega, N.; Salvador, P.; Dannenberg, J. J.; Malick, D. K.; Rabuck, A. D.; Raghavachari, K.; Foresman, J. B.; Cioslowski, J.; Ortiz, J. V.; Baboul, A. G.; Stefanov, B. B.; Liu, G.; Liashenko, A.; Piskorz, P.; Komaromi, I.; Gomperts, R.; Martin, R. L.; Fox, D. J.; Keith, T. A.; Al-Laham, M. A.; Peng, C. Y.; Nanayakkara, A.; Challacombe, M.; Gill, P. M. W.; Johnson, B. G.; Chen, W.; Wong, M. W.; Andres, J. L.; Gonzalez, C.; Head-Gordon, M.; Replogle, E. S.; Pople, J. A.; Gaussian, Inc.: Pittsburgh, PA, 2002.
(42) Hariharan, P. C.; Pople, J. A. *Chem. Phys. Lett.* **1972**, *16*, 217.
(43) Stevens, P. J.; Devlin, J. F.; Chabalowski, C. F.; Frisch, M. J. *J. Phys. Chem.* **1994**, *98*, 11623.
(44) Dewar, M. J. S.; Zoebisch, E. G.; Healy, E. E.; Stewart, J. J. P. *J. Am. Chem. Soc.* **1985**, *107*, 3902.
(45) Dewar, M. J. S.; Zoebisch, E. G. *J. Mol. Struct. (THEOCHEM)* **1988**, *49*, 1.
(46) Dewar, M. J. S.; Yate-Ching, Y. *Inorg. Chem.* **1990**, *29*, 3881.
(47) Chambers, C. C.; Hawkins, G. D.; Cramer, C. J.; Truhlar, D. G. *J. Phys. Chem.* **1996**, *100*, 16385.
(48) Kofranek, M.; Kovar, T.; Karpfen, A.; Lischka, H. *J. Chem. Phys.* **1992**, *96*, 4464.
(49) Millefiori, S.; Alparone, A. *J. Chem. Soc., Faraday Trans.* **1998**, *94*, 25.
(50) Benincori, T.; Brenna, E.; Sannicolo, F.; Zotti, G.; Zecchin, S.; Schiavon, G.; Gatti, C.; Frigerio, G. *Chem. Mater.* **2000**, *12*, 1480.
(51) Orti, E.; Sanchez-Marin, J.; Tomas, F. *Theor. Chim. Acta* **1986**, *69*, 41.
(52) Karpfen, A.; Choi, C.-H.; Kertesz, M. *J. Phys. Chem. A* **1997**, *101*, 7426.
(53) Arulmozhiraja, S.; Fujii, T. *J. Chem. Phys.* **2001**, *115*, 1058910595.
(54) Cramer, C. J. *Essentials of Computational Chemistry: Theories and Models*; John Wiley & Sons: New York, 2002.
(55) Cramer, C. J.; Truhlar, D. G. *Chem. Rev.* **1999**, *99*, 2161.
(56) Curutchet, C.; Cramer, C. J.; Truhlar, D. G.; Ruiz-Lopez, M. F.; Rinaldi, D.; Orozco, M.; Luque, F. J. *J. Comput. Chem.* **2003**, *24*, 284.
(57) Chuang, Y.-Y.; Radhakrishnan, M. L.; Fast, P. L.; Cramer, C. J.; Truhlar, D. G. *J. Phys. Chem. A* **1999**, *103*, 4893.
(58) Rinaldi, D.; Rivali, J.-L. *Chem. Phys.* **1973**, *32*, 57.
(59) Miertus, S.; Scrocco, E.; Tomasi, J. *J. Chem. Phys.* **1981**, *55*, 117.
(60) Storer, J. W.; Giesen, D. J.; Cramer, C. J.; Truhlar, D. G. *J. Comput.-Aided Mol. Des.* **1995**, *9*, 87.
(61) Li, J.; Zhu, T.; Cramer, C. J.; Truhlar, D. G. *J. Phys. Chem. A* **1998**, *102*, 1820.
(62) Lu, X.-J.; Olson, W. K. *Nucl. Acids Res.* **2003**, *31*, 5108.
(63) Berman, H. M.; Olson, W. K.; Beveridge, D. L.; Westbrook, J.; Gelbin, A.; Demeny, T.; Hseih, S.-H.; Srinivasan, A. R.; Schneider, B. *Biophys. J.* **1992**, *63*, 751.
(64) Berman, H. M.; Zardecki, C.; Westbrook, J. *Acta Crystallogr.* **1998**, *D54*, 1095.
(65) Shui, X.; McFail-Isom, L.; Hu, G. G.; Williams, L. D. *Biochem.* **1998**, *37*, 8341.
(66) Olson, W. K.; Bansal, M.; Burley, S. K.; Dickerson, R. E.; Gerstein, W.; Harvey, S. C.; Heinemann, U.; Lu, X.-J.; Neidle, S.; Shakked, Z.; Sklenar, H.; Suzuki, M.; Tung, C.-S.; Westhof, E.; Wolberger, C.; Berman, H. M. *J. Mol. Biol.* **2001**, *313*, 229.